

pubs.acs.org/ac Article

Quantitative Recoveries of Exosomes and Monoclonal Antibodies from Chinese Hamster Ovary Cell Cultures by Use of a Single, Integrated Two-Dimensional Liquid Chromatography Method

Sarah K. Wysor and R. Kenneth Marcus*



Cite This: Anal. Chem. 2023, 95, 17886-17893



ACCESS I

III Metrics & More

ABSTRACT: Cultured cell lines are very commonly used for the mass production of therapeutic proteins, such as monoclonal antibodies (mAbs). In particular, Chinese hamster ovary (CHO) cell lines are widely employed due to their high tolerance to variations in experimental conditions and their ability to grow in suspension or serum free media. CHO cell lines are known for their ability to produce high titers of biotherapeutic products such as immunoglobulin G (IgG). An emergent alternative means of treating diseases, such as cancer, is the use of gene therapies, wherein genetic cargo is "packaged" in nanosized vesicular structures, referred to as "vectors". One particularly attractive vector option is extracellular vesicles (EVs), of which exosomes are of greatest interest. While exosomes can be harvested from virtually any

Exosomes retained Light Scattering Detection of Exosomes

Cell Culture Supernatant

IgG

retained

Add with Biorende

Article Recommendations

human body fluid, bovine milk, or even plants, their production in cell cultures is an attractive commercial approach. In fact, the same CHO cell types employed for mAb production also produce exosomes as a natural byproduct. Here, we describe a single integrated 2D liquid chromatography (2DLC) method for the quantitative recovery of both exosomes and antibodies from a singular sample aliquot. At the heart of the method is the use of polyester capillary-channeled polymer (C–CP) fibers as the first dimension column, wherein exosomes/EVs are captured from the supernatant sample and subsequently determined by multiangle light scattering (MALS), while the mAbs are captured, eluted, and quantified using a protein A-modified C–CP fiber column in the second dimension, all in a 10 min workflow. These efforts demonstrate the versatility of the C–CP fiber phases with the capacity to harvest both forms of therapeutics from a single bioreactor, suggesting an appreciable potential impact in the field of biotherapeutics production.

Chinese hamster ovary (CHO) cells are popular cell lines due to their capabilities in the large-scale production of therapeutic monoclonal antibodies (mAbs) in suspension and serum-free media.^{1,2} These cell lines are also desirable because of their high tolerance to variations in growth conditions, including temperature, pH, and pressure.^{3,4} In many cases, the mAb immunoglobulin G (IgG) is the desired biopharmaceutical therapeutic product, where there is a need for the isolation, quantification, and characterization of the IgG throughout the production and recovery cycles. IgG is excreted from the cells, where it can be found in the cell culture supernatant along with other contaminants, such as host cell proteins (HCPs), DNA, virus particles, and other cell secretion products⁶⁻⁸; therefore, intense downstream processing is required for their isolation and further characterization.^{9,10} The most common, yet costly method for isolation of IgG is protein A (ProA) chromatography due to its ability to selectively capture and quantify IgG. ProA columns consist of a Staphylococcus aureus (SPA)modified stationary phase that allows for the specific binding of IgG, as there are five sites on SPA that bind with the Fc region on IgG. 11,12 Alternative IgG purification/isolation approaches have included cation exchange chromatography (CEX)^{13,14}

and size exclusion chromatography (SEC), ¹⁵ which are also useful for isolating IgG charge variants and aggregation, respectively. However, these methods still require ProA chromatography for the selective isolation of IgG among the prevalent HCPs. Primary issues with commercial, analytical-scale ProA columns are their high cost (\sim \$1500 for 0.10 mL bed volume) and the fact that the columns can degrade over time due to the harsh elution (i.e., low pH \sim 2) and regeneration (i.e., \sim 1 M NaOH) conditions.

While IgG is the commonly desired therapeutic product from cell lines, another approach to treat diseases is through gene therapies, which implement vectors that encapsulate the therapeutic agents, delivering genetic, and proteinaceous material to specific cells to alter the way they function.¹⁶ The most common of the vector systems under development

Received: September 8, 2023 Revised: October 18, 2023 Accepted: November 10, 2023 Published: November 23, 2023





are adeno-associated viruses (AAVs), 17 lentiviruses, 18 lipid nanoparticles (LNPs), 19 and exosomes. 20 Exosomes, a subset of the extracellular vesicles (EVs), have recently gained attention as vectors due to the plethora of natural sources from which they can be harvested and/or cultured.21-Exosomes are 50-200 nm in size with a phospholipid bilayer that encapsulates biomolecular contents from the host cell of origin. Due to their makeup, exosomes are intimately involved in cellular communication 20,25,26 and thus can be used as vectors, being proven to be capable of tissue-specific delivery and crossing biological barriers, such as the blood brain barrier. 25,27 In comparison to current vectors, exosomes are advantageous due to their biocompatibility, easy uptake without negative immune responses, lower toxicity, and selectivity toward target cancer cells.²⁸ Exosomes have been used to treat various cancers ranging from ovarian to pancreatic cancers, ²⁹⁻³³ with tumor-derived exosomes proven to target the cell-types of origin.²⁸ Recent studies have also looked at engineering exosomes for the targeted transport of their contents. 26,34 At present, a number of different cell cultivation approaches are under investigation for mass production, including those derived from human mesenchymal stem cells (MSCs) and embryonic kidney (HEK) cells³⁵ as well as CHO cells.³⁶ As exosomes are a natural byproduct of CHO cell culturing, in principle, the same bioreactor could be used for the large-scale production of two therapeutic products: exosomes and mAbs.

Current exosome isolation methods include ultracentrifugation (UC),^{37,38} size exclusion chromatography (SEC),³ anion exchange chromatography (AEX), 34,41 and a variety of polymer-based precipitation methods. 42,43 UC is the most and a variety of commonly employed method at the bench level, even though it is capital-expensive with long, multistage processing times and low purity exosome isolates. These characteristics are severely exacerbated when scale-up is considered for vector production. SEC, and to a much lesser extent AEX, approaches have been growing in use, but the hydrodynamic volume-based and charge-based separations, respectively, result in the coelution of non-EV species such as lipoproteins, low purity recoveries, and require additional postisolation UC steps. Finally, while readily implemented, precipitation methods result in low purity, with the resulting exosome precipitate containing free proteins. 44,45 As is common with the isolation of protein-based therapeutics (i.e., mAbs), the use of unit operation, chromatography-based exosome processes would de facto provide potential benefits with regard to lower capital costs, high levels of throughput and automation, and the integration of in-line means of detection/quantification.

This laboratory has extensively reported on the use of novel-shaped polymer fibers, capillary-channeled polymer (C–CP) polymer fibers, as stationary phases for the high-efficiency separation of proteins. He commodity-scale base polymers are melt-extruded into 8-pronged or trilobal cross section shapes, with the base fiber materials having a range of decreasing hydrophobicity from polypropylene (PP), to polyester (PET), and nylon, with options for modification. Due to the variety of surface chemistries offered, C–CP fibers have been implemented across a variety of separation modalities including reversed phase (RP), He ion exchange (IEX), He ion exchange (IEX

 μ m diameter open capillaries when packed into column format, resulting in very low mass transfer resistance and reduced backpressure at high linear flow velocities. 46,57 More recently, columns and spin-down tips consisting of PET C-CP fibers have been demonstrated toward the rapid and effective isolation of exosomes from matrices ranging from human urine, plasma, and breastmilk, and CHO- and HEK-cell culture supernatants as well as 20 different plant materials, via an HIC capture/elution method. 58-63 The HIC separation utilizes high-to-low salt concentration gradients along with the introduction of an organic modifier to assist in eluting the species within 10 min separation times and yielding high purity EV eluates. The capture efficiency, product purity, processing times, and operational costs have been determined, and compare extremely well to the previously cited EV isolation methodologies.64

While efficient isolations of IgG and exosomes have been demonstrated independently from CHO cell supernatants on PP C-CP fibers modified with ProA⁵²⁻⁵⁴ and via HIC on native PET fibers, 65 respectively, the simultaneous production of both entities in the same bioreactor begs the question as to how both species might be efficiently produced and harvested, providing greater overall pharmaceutical yields from the same bioprocess. As EV production is known to reflect the stress/ productivity of cell lines, 66,67 it may be that the dual-analysis capability could contribute as a means of providing fundamental insights or as a process monitoring tool.⁶⁸ Here, we report what is believed to be the first isolation of EVs and IgG from a single aliquot of the CHO supernatant using 2DLC coupling HIC x ProA isolations. A very novel means of solvent mismatch compensation is affected with both species concentrations readily determined. For each isolation, C-CP fiber support and stationary phases are implemented. For the 2DLC method presented here, the PET and ProA-derivatized PP C-CP columns are employed, respectively. The first dimension (¹D) incorporates HIC for the isolation of EVs, while the second dimension (2D) ProA column captures and isolates IgG for its quantification. Multiangle light scattering (MALS) is applied in-line with ¹D for the sizing and quantification of the EVs. Initially, heart-cut and comprehensive methods were considered for the transfer of the ¹D eluate, but IgG retention on the ²D ProA column proved to be challenging. To improve the IgG retention, the ProA column was placed in the loop of the switch valve acting to continuously integrate all of the IgG passing through the HIC phase. With this configuration, the ProA column can be implemented in-line with ¹D and ²D, and in fact, a further column chromatography step could be employed in ²D. Small EVs/exosomes of characteristic sizes were observed via transmission electron microscopy (TEM) and MALS, with the EVs falling between 15-400 nm in diameter, with the majority (50%) falling between 75 and 210 nm. Additionally, EV particle concentrations were determined using MALS, with a value of 3.33×10^{10} particles per mL of the original supernatant determined. IgG quantification eluting from the ProA column was performed via an absorbance spectrophotometry response curve covering 20-300 µg of on-column injection with an R^2 of 0.9983. With both EVs and IgG being present in CHO cell culture supernatants, this novel method presents a rapid, cost-effective means of isolating and quantifying these two therapeutic agents from a single cell culture source.

MATERIALS AND METHODS

Chemicals and Sample Preparation. Sodium phosphate, monobasic, monohydrate (EMD Millipore, Merck, Germany), sodium phosphate, dibasic (MilliporeSigma, Merck, Germany), sodium chloride (MilliporeSigma, Merck, Germany), citric acid (MilliporeSigma, Merck, Germany), ammonium sulfate (ThermoScientific, MA, USA), Gibco phosphate buffered solution (PBS) 10× pH 7.4 (ThermoScientific, MA, USA), and acetonitrile (ACN) (VWR, PA, USA) were used for mobile phase preparations. Deionized water (DI-H2O) was obtained from an Elga PURELAB flex water purification system, (18.2 MΩ-cm, Veolia Water Technologies, High Wycombe, England). Silica standards (NanoFCM, Nottingham, UK) were used for confirmation of vesicle sizing and concentration via MALS. Native recombinant S. aureus Protein A (rSPA) (animal free) (Syd Laboratories, Hopkinton, MA) was used for ProA C-CP column preparation. Pure immunoglobulin G (IgG) (MilliporeSigma, Merck, Germany) was used as a standard for the ProA separations, with absorbance detection used to quantify the antibodies. The Chinese hamster ovary (CHO) cell supernatant from a CHO K1 cell line was obtained from the Harcum laboratory (Department of Bioengineering, Clemson University). The CHO cell culture was grown in 125 mL shake flasks in suspension with 30 mL of EX-CELL CD CHO serum free medium (Cat. No. 14361C) in a humidified incubator containing 5% CO2 at 37 °C, shaken at 100 rpm. The supernatant was centrifuged at 1000g and stored at −20 °C prior to use. Before use, the supernatant was filtered using a $0.22 \mu m$ poly(ether sulfone) (PES) filter.

Column Preparation. Polyester (PET) and polypropylene (PP) C-CP fibers were extruded by the Department of Material Science and Engineering at Clemson University, with the columns prepared as previously described.⁶⁹ The fibers were pulled through poly(ether ether ketone) (PEEK) tubing (0.76 mm inner diameter) and trimmed to 30 cm. The columns were mounted in the HPLC systems and washed with DI-H₂O, followed by ACN and then again by DI-H₂O until a stable background absorbance response was achieved to remove any antistatic coatings from the extrusion process. As described previously, the hydrophobic, slightly anionic nature of the PET fibers is such that they are used in their native state for the HIC isolation of exosomes. 59,65 The PP fiber C-CP column was modified to create a ProA column by passing a 0.5 mg mL⁻¹ solution of rSPA through the column at a rate of 0.5 mL min⁻¹ for ~6 min to achieve column saturation, as described previously.52

Instrumentation. An Agilent 2D HPLC (Agilent Technologies, Santa Clara, CA) was used for all chromatographic measurements, with a stack consisting of 1 D: 1260 binary pump, 1260 degasser, 1100 multiple wavelength detector, 1290 valve drive, 2 D: 1290 UHPLC high-speed pump, and 1290 variable wavelength detector, all controlled under the ChemStation operating system. Light scattering measurements of the exosome eluates were recorded with an in-line DAWN MALS detector (Wyatt, Santa Barbara, CA, USA) controlled by ASTRA software. The dn/dc value for exosomes was set as 0.1850, and the refractive index of exosomes for particle sizing was 1.51. The refractive index of the eluate was experimentally determined to be 1.34649 by a Reichert AR7 Series Automatic Refractometer at 22 °C in the 40% ACN eluate in 1× PBS. Transmission electron microscopy (TEM) was performed

using a Hitachi HR7830, using the same sample preparation method as previously reported.⁶⁴

Methods. Individual separations were performed before coupling the two modalities for comprehensive 2DLC separations. For the 3-step HIC separation, 65 the mobile phases include 2 M ammonium sulfate in 1X PBS and 40% ACN in 1× PBS. The sample is injected under 2 M ammonium sulfate (held for 5 min), where salts and sugars are passed unretained. The second step elutes proteins by reducing the salt concentration and adding an organic modifier; 1 M ammonium sulfate and 25% ACN in 1× PBS (held for 5 min). Finally, the third step elutes EVs using 40% ACN in 1× PBS (held for 5 min). Standalone HIC separations were performed at 0.5 mL min⁻¹. For the ProA separations, 50 mM sodium phosphate (a mixture of mono and dibasic to achieve pH = 7.4) as the binding buffer, and 150 mM citric acid (pH = 2.6) as the elution buffer. ProA separations were performed at a flow rate of 1.0 mL min⁻¹. Optical absorbance at 216 and 280 nm was used to monitor the separations.

Initially, for the 2DLC coupling, the HIC and ProA columns were placed in the standard ¹D and ²D positions, respectively, coupled by the ²D injection loop. The flow rate of the ¹D HIC separation was 0.1 mL min⁻¹, with a flow rate of 1.0 mL min⁻¹ employed for the ²D ProA separation. The sample was introduced in 2 M ammonium sulfate (held for 4 min), followed by protein elution with 1 M ammonium sulfate +25% ACN (held for 20 min). The protein fraction of the HIC separation was then comprehensively transferred to the ²D ProA column into 50 mM sodium phosphate (pH = 7.4). The IgG was eluted using 150 mM citric acid (pH 2.6) and held for 6 min.

A graphic depiction of the second (adapted) 2DLC column configuration is presented in Figure 1. The HIC column is placed in the ¹D, while the ProA column was placed in the position of the transfer loop of the 2DLC instrumentation, similar to a study previously reported using a fiber column as a capture loop. ⁷⁰ (The flexible column is mounted literally in the place of the ²D injector loop.) Initially, the HIC and ProA

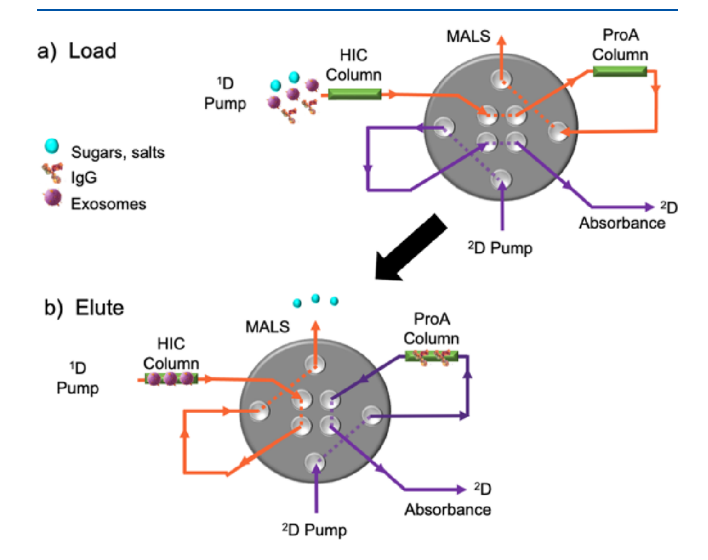


Figure 1. Diagrammatic representation of the 2DLC coupling of the C–CP fiber HIC and ProA columns for the isolation of exosomes and IgG from CHO cell culture supernatants. (a) Fluid path for the initial sample introduction and (b) valving for the elution of the respective column isolates.

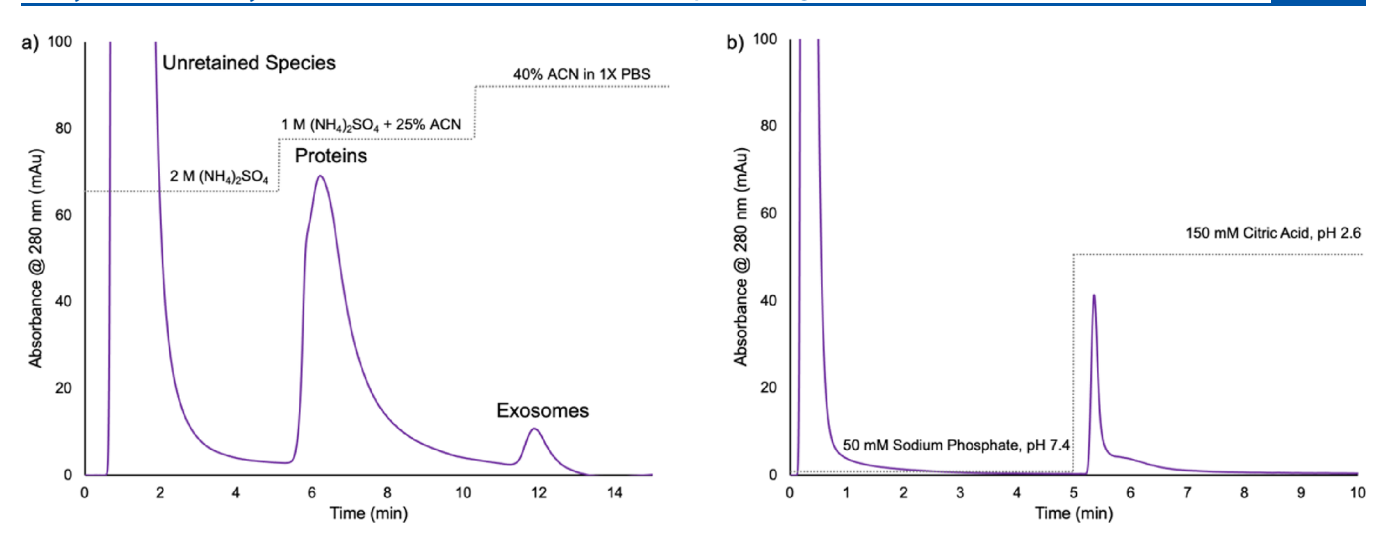


Figure 2. Demonstrative chromatographs for the individual isolation and recovery processes employed for the isolation of therapeutics from CHO cell culture supernatants. (a) Chromatogram of 3-step HIC isolation of exosomes. The sample is introduced in 2 M ammonium sulfate, where salts and sugars are unretained. Proteins are eluted around 6 min with 1 M ammonium sulfate and 25% ACN in 1X PBS, and exosomes are eluted around 12 min with 40% ACN in 1X PBS. (b) Chromatogram of ProA isolation of IgG, with sample injected in 50 mM sodium phosphate, pH 7.4, and IgG elution with 150 mM citric acid, pH 2.6. In each case, a 20 µL supernatant aliquot is injected.

columns are inline in ¹D (Figure 1a, orange path), where the sample is injected under the protein elution conditions for HIC (1 M ammonium sulfate and 25% ACN) and held for 2 min. In this situation, small molecules, salts and proteins pass the HIC column unretained, and the EVs are retained on the PET fibers, while the IgG is subsequently retained on the ProA column in the switch valve loop as the salts etc. pass to waste. The HIC and ProA separations were performed at flow rates of 0.5 and 1.0 mL min⁻¹, respectively. At time = 2 min, the ProA column is transferred to the path of ²D (Figure 1b, purple path) and equilibrated with 50 mM sodium phosphate (pH 7.4) (2-4 min). While the 2D column is equilibrating, the EVs are eluted from the ¹D using 40% ACN in 1× PBS. IgG is eluted from the ProA column with 150 mM citric acid (pH 2.6) (4-6 min). The MALS detector was placed in-line with the ¹D for exosome sizing, while the ProA eluate was passed through the absorbance detector. Prior to each separation sequence, the HIC column was re-equilibrated in 1 M ammonium sulfate +25% ACN and the ProA column in 50 mM sodium phosphate (pH = 7.4).

RESULTS AND DISCUSSION

Individual Separation Modalities. Prior to the effect of the combined, 2D exosome/IgG separation, the efficacy of the individual separations on the respective C-CP columns was verified. HIC separations have been previously used by Marcus et al. for protein and EV isolations due to their nondenaturing elution conditions in comparison to other modes of chromatography. 48,55,56,65 The resulting chromatogram for the composite 3-step gradient HIC separation of CHO cell supernatant constituents is presented in Figure 2a. The sample is injected onto the PET column in 2 M ammonium sulfate (0-5 min), where salts, sugars, and polar small molecules pass through the column (unretained) due to their hydrophilic nature. In this solvent, the proteins and EVs are retained due to the salt's disruption of the water layer surrounding the analytes and exposing the hydrophobic sites.⁷¹ A solvent gradient step is taken to elute the proteins (5-10 min) by lowering the salt concentration and adding ACN as an organic modifier, which

weakens the hydrophobic nature of the protein—fiber interaction,⁷² while the decrease in salt content increases the water barrier around the proteins to promote elution. Finally, the EVs, the most hydrophobic species, are eluted in the step initiated at 10 min, where the salt is eliminated and the solvent consists of 40% ACN in PBS.

ProA separations are commonly used for IgG purification because of their specificity toward IgG retention. 11,12 ProA separations have also been previously performed on modified PP C-CP fiber columns, with detailed studies of ProA loading, IgG binding capacities and practical applications described. 52-54 As is common in all IgG bind-and-elute protocols, a step gradient utilizing a pH drop was employed here with a representative chromatogram shown in Figure 2b. Here CHO cell supernatant is introduced and IgG captured onto the modified column in a 50 mM sodium phosphate buffer (pH = 7.4) and eluted with 100 mM citric acid (pH = 2.6). At a pH of \sim 7, the Fc regions of the IgG are exposed and can bind to the five potential binding domains present on protein A, with a typical binding capacity of two IgG per ligand molecule.⁷³ The IgG binding site is hydrophobic in nature, with hydrogen bonding and electrostatic interactions implicated in the interaction. ^{74,75} The IgG is eluted at a pH of \sim 2, which causes the IgG molecule to fold in on itself with the Fc binding sites being no longer accessible. The IgG is seen here to elute as a fairly well-defined plug, with some tailing observed due to higher-order interaction that may be occurring at the fiber surface.

2D HIC x ProA with Comprehensive Transfer. The motivation for coupling HIC and ProA chromatographic modalities is to provide a single platform method for the isolation and characterization of two therapeutic products (exosomes and mAbs) from a single source (e.g., a CHO cell supernatant) in a high throughput process. As shown in Figure 2, the HIC and ProA separations can address the isolation of each of these analytes; therefore, coupling the two on a single 2D chromatographic platform would seem to be a practical approach; so long as the pairing provides the same level of separation quality. As depicted in Figure 1, the HIC column is implemented in ¹D followed by ProA column in ²D. As is true

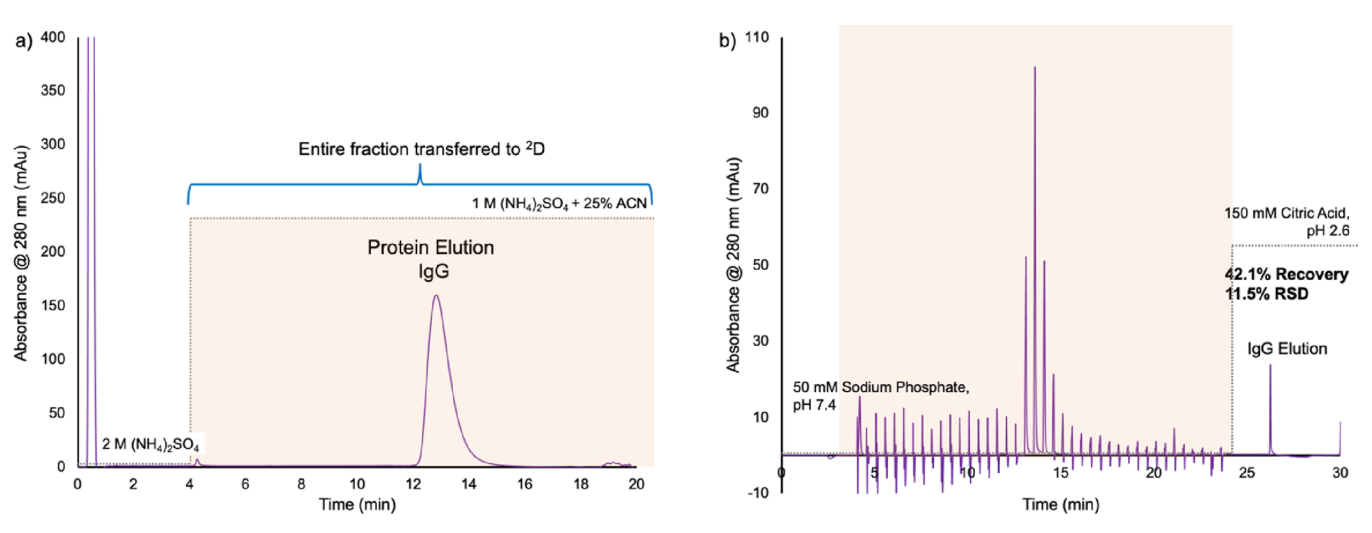


Figure 3. (a) Chromatogram of the elution of the protein fraction of CHO cell supernatant from the PET C–CP fiber column under HIC conditions. Injection conditions: 2 M ammonium sulfate; elution conditions: 1 M ammonium sulfate +25% ACN. The entire fraction of protein elution is comprehensively transferred to 2 D. (b) Chromatogram obtained at the exit of the 2 D ProA C–CP fiber column. Comprehensive transfer with an 80 μL injection loop at intervals of 0.5 min. Injection mobile phase 50 mM sodium phosphate, pH 7.4 from 0–23 min. Elution of captured IgG initiated at 26 min with 150 mM citric acid, pH 2.6. The orange-shaded portions in each chromatogram represent the transfer fraction from 1 D to 2 D.

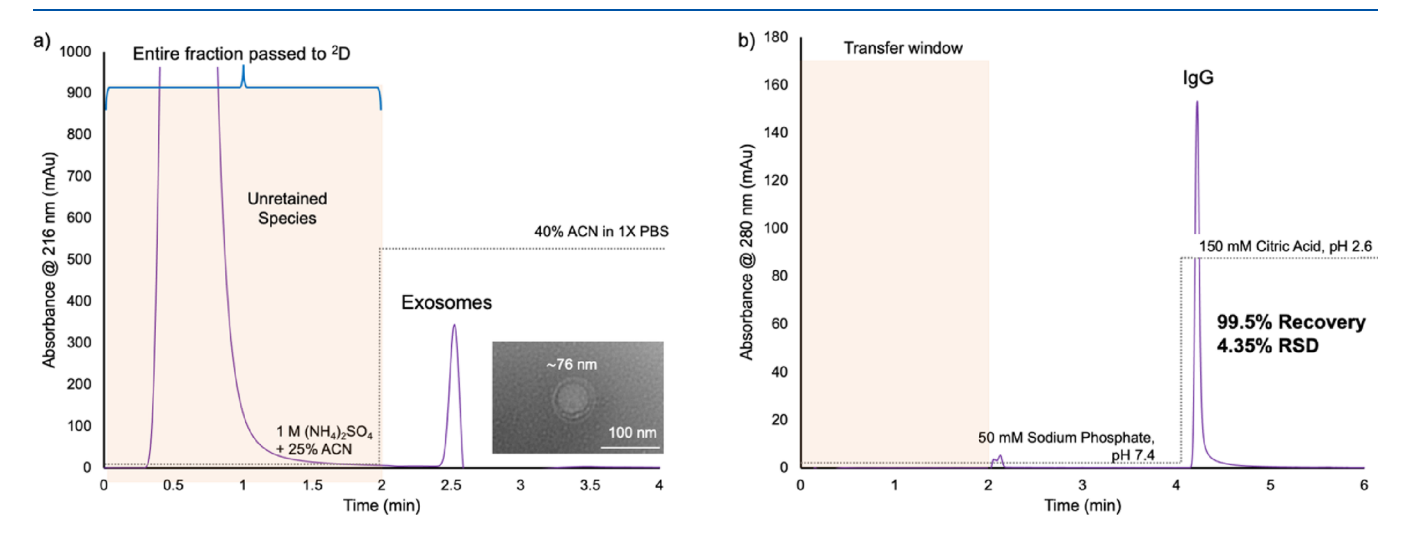


Figure 4. Product chromatograms for the separate stages of the isolation of a) exosomes and b) IgG from a 20 μ L injection of CHO cell culture supernatant. (a) 1 D HIC isolation of exosomes with absorbance detection. TEM image of a single exosome (magnification = ×100.0K, acc. voltage = 120.0 kV). (b) 2 D ProA isolation of IgG with column placed in the switch valve loop and absorbance detection. The orange region of each chromatogram represents the time frame where the two columns are in-line with each other.

in virtually all 2DLC couplings, there are many practical considerations in the method development, including solvent compatibilities, column-to-column transfer conditions, and the ever-present set of tradeoffs between chromatographic resolution, sensitivity, etc. (e.g., heart-cut versus comprehensive sampling). These aspects are particularly complex in the case of 2DLC protein separations. The primary challenges in this specific application include the potential effects of the HIC elution solvent composition, the sampling approach, and the effects of the pH on IgG capture/release.

Initially, the entire protein fraction of the 3-step HIC separation was transferred to the 2D ProA column through a comprehensive transfer method, employing an 80 μ L sampling loop to introduce the 1D eluates to the second dimension ProA column at 0.5 min intervals. As shown in Figure 3a, the introduction of pure IgG under high salt conditions followed by elution from the HIC column with the 1 M $(NH_4)_2SO_4/$

25% ACN solvent, provides a well-defined band for introduction into the ²D ProA C-CP column. Figure 3b is a chromatogram recorded at the exit of ²D, with the time axis being the same as in Figure 3a, with the acidic IgG wash step from that column initiated at 24 min. Seen in the time frame of the HIC passage and ProA accumulation steps are a series of pulses at 0.5 min intervals reflective of solvent mismatches between the HIC elution solvent and the 50 mM sodium phosphate ²D mobile phase. Also seen at times equivalent to the IgG elution from ¹D is an absorbance representative of IgG that is not retained on the ProA column. Finally, the citric acid elution from the ProA column yields a well-defined response for the antibody. The extended protein elution time is due to the lower flow rate (0.1 mL min⁻¹) required for the comprehensive transfer (i.e., continuous transfer) from ¹D to ²D. A comparison of the integrated peak area for the IgG elution band versus the standard injected without a column

present reveals an average recovery of only 42.1% with a variability of 11.5% RSD. The nonquantitative recovery of the IgG is attributed to the binding and elution of the IgG from the HIC column, first resulting in less retention on the ProA column as exhibited in the breakthrough in the 13-16 min portions of the chromatogram of Figure 3b. Separate studies revealed little perturbation in the recoveries upon exposure to the ACN in the ¹D elution solvent, so the lack of retention is attributed to the period of time that the IgG molecules were first adsorbed to the PET fiber surface, wherein they have a tendency to denature and fold onto themselves. In this way, the hydrophobic sites responsible for the specific interaction between ProA and the Fc region of IgG are not available. 74,75 In actuality, it cannot be ruled out that the presence of ACN while the eluate was in the injection loop exacerbated this problem. With these results, a new approach to this 2DLC coupling was needed.

HIC x ProA Capture Loop Coupling. As the adsorption and desorption of IgG on the HIC column played a role in perturbing its targeted retention to the ProA column, a new approach was established. Ideally, the initial HIC step could be performed to isolate the EVs, but not cause IgG to be adsorbed. In fact, previous works have shown the ability to isolate and purify EVs from proteins when injecting the sample under the normal "protein elution" conditions (i.e., all proteins flow through and EVs are retained). 61 To prevent the surface denaturation holdup time of IgG in the organic solvent, the placement of the flexible ProA column was changed to the position of the switch valve loop. Moving forward, the 3-step HIC separation was reduced to a 2-step separation. With the two-step separation, the CHO supernatant sample is introduced under protein elution conditions, where the solvent is 1 M ammonium sulfate and 25% ACN. Under these solvent conditions, small molecules, salts, and proteins (including IgG) present in the CHO cell supernatant flow through unretained, while the EVs are retained. The passthrough continues on to the in-line ProA column. The EVs can be subsequently eluted from the PET column, as before, using 40% ACN, represented by the peak around 2.5 min in the chromatogram of Figure 4a. To confirm the morphology and presence of EVs from the single-step HIC separation, TEM was performed on the exosome eluates. As shown in the inset of Figure 4a, exosomes of characteristic size and shape were observed, with the phospholipid bilayer easily distinguished.

As depicted in Figure 4a and continued in Figure 4b, the entirety of the ¹D passthrough was introduced for 2 min through the ProA column for IgG recovery. As demonstrated previously, the ProA C-CP fiber columns are very effective in selectively pulling IgG from supernatant solutions, 52,53 with the nontargeted species simply passing through unretained to waste. In practice, as long as a situation of column overload is not reached, the entire IgG population is captured (integrated) on the ProA column. As depicted in Figure 4b, at the time of 4 min (inclusive of the initial HIC step), the switch valve is changed so that the ProA column is in line with the ²D (Figure 1b) to elute the IgG for subsequent quantification. The species unretained on the ProA column are not observed in the chromatogram as the ProA column is in line with the waste and no detector at this point. Again, the recovery of IgG for this column placement was determined by injecting an IgG standard with and without the HIC column present in the ¹D. The recovery of IgG using the 2-step HIC method was 99.5, with a n = 3 precision of 4.35% RSD, demonstrating excellent

recovery and reproducibility. Based on this complete 2D configuration for the separation, a response curve was created for on-column injections ranging from 20 to 300 μ g of IgG. Based on the elution peak area responses at 280 nm, a response curve of y=0.449x+0.0119 having an R^2 value of 0.9983 was obtained. Using this response curve from neat IgG solutions, a 20 μ L CHO cell supernatant sample was introduced for quantification. The supernatant was determined to contain 179 μ g mL⁻¹ IgG, agreeing well with the targeted ~2 mg mL⁻¹ productivity value for that particular bioreactor program.

As depicted in the chromatogram of Figure 4a, the exosome fraction of the CHO cell supernatant is cleanly eluted from the PET fiber HIC column. Previous works from this laboratory have demonstrated the efficacy of using standard HPLC absorbance (actually scatting) detection approaches to quantify exosomes. Multiangle light scattering (MALS) is envisioned as a complementary detection modality to absorbance, as it has the inherent capacity to provide particle/vesicle sizing and number densities. In this case, the ¹D exosome eluate was passed through the MALS detector with the results of the sizing experiments shown in Figure 5. As

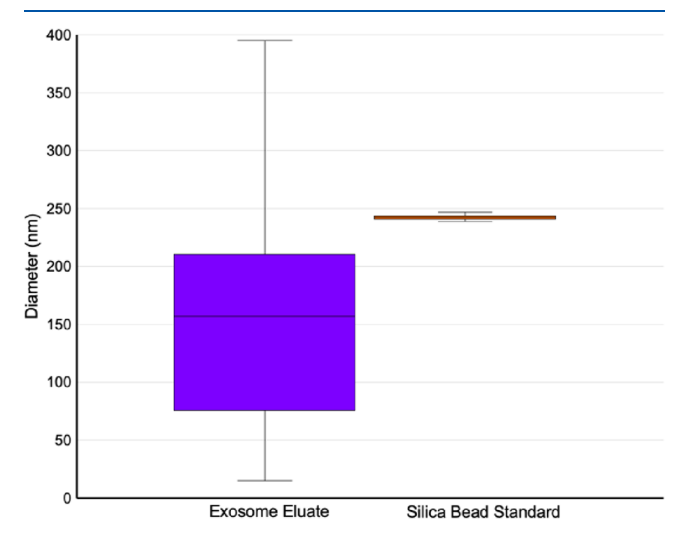


Figure 5. Multiangle light scattering (MALS) sizing of CHO cell-supernatant-derived EVs following HIC separation. Diameters of EVs ranged from 15–395 nm with a mean of 157 nm. Silica bead standard exhibits diameters ranging from 239–247 nm, in good agreement with known values.

shown in the figure, the CHO cell exosomes yield sizes ranging from \sim 15–400 nm in diameter, with 50% of the sizes falling between 74 and 210, in agreement with postisolation determinations for CHO cell supernatants, ranging from ~30-300 nm.81 To confirm the sizing determination, the particle diameters for a silica standard were also determined with an expected diameter of 230-260 nm and confirmed via MALS with experimental values between 233 and 251 nm here, also shown in Figure 5. The same silica bead standard was used to calibrate the MALS response relative to particle counting/concentration. The specific standard solution was prepared to a nominal concentration of $\sim 1.6 \times 10^{10}$ particle mL⁻¹, which had a measurement precision of 4.5% RSD for triplicate measurements. Triplicate aliquots of the CHO cell supernatants yielded exosome densities of 3.3×10^{10} mL⁻¹, with a variability of 9.7% RSD for the complete separation process. The concentration determined here, is in line with

other EV concentration determinations in CHO supernatant, 82 which are known to vary with cell culture conditions and the growth day/stage of supernatant harvest.

CONCLUSIONS

Mammalian cell cultures are the standard means by which therapeutic antibodies are produced. While monoclonal antibodies are the most common means of treating many diseases, there has been explosive growth in the development of different vector entities for targeted therapeutic delivery. Among the suit of vectors, exosomes hold particular promise due to their low immunotoxicity, large cargo capacities, and ready production from the standard mammalian cell line. Here, we demonstrate a singular, two-dimensional liquid chromatography (2DLC) platform that allows for the isolation and quantification of both exosomes and the monoclonal antibody IgG from a single cell culture supernatant sample. This 2DLC method employs a PET C-CP fiber column to isolate the exosome population with the passthrough of that column introduced to a ProA-derivatized PP C-CP fiber column. Both stages yield well-defined bands of the targeted species for detection and quantification.

Exosomes were captured and isolated in ¹D with two-step HIC separation, with the particle number density and sizing determined via MALS, with a high level of precision and with values well in line with expectations. TEM imaging validated the integrity of the vesicular structure and sizing. Following the HIC column, the ProA column was placed in the switch valve loop usually employed for sample introduction into the ²D of a standard 2DLC system. The ProA column serves to integrate the eluting IgG, with the use of standard absorbance detection yielding overall recoveries of >99% and precision on the level of 4% RSD. Ultimately, the entire separation process is achieved in less than 5 min for the two biotherapeutic species.

The approach demonstrated here would seem to have many positive implications with regard to the study of cell culture processes, process analytical technologies, and the field of downstream processing in the biopharmaceutical industry. In particular, as exosomes and monoclonal antibodies are coproducts in mammalian cell culture processes, the possibility exists to generate and recover both forms of therapeutics from a singular reaction vessel. A second product for only the cost of the purification method from a singular cell culture process would be a positive outcome. While there likely would be different culture conditions that are tailored to one or the other product, 35,83 this capability addresses an untapped resource in any case. The data of the sort presented here would be a key component in such process developments. Future work will include aspects aligned with cell culture process scale-up as well as analytics. Regarding scaleup, efforts are now underway toward moving the C-CP fiber column technology to the preparative scale. Initial efforts in determining the dynamic binding capacities toward EV and mAb isolation suggest great ⁴ with the ability to easily scaleup the column capacities using very straightforward scaling laws and approaches regarding column dimensions. 10 In terms of analytics, as only one stage of the 2DLC pumping is utilized with these coupled columns, an additional column could be inserted in the available ²D stage, such as weak cation exchange or size exclusion chromatography could be employed to evaluate antibody charge variants or extent of aggregation, respectively. Ultimately, this straightforward approach will

provide advantages in terms of information content, throughput, and costs.

AUTHOR INFORMATION

Corresponding Author

R. Kenneth Marcus — Department of Chemistry, Biosystems Research Complex, Clemson University, Clemson, South Carolina 29634-0973, United States; orcid.org/0000-0003-4276-5805; Email: marcusr@clemson.edu

Author

Sarah K. Wysor – Department of Chemistry, Biosystems Research Complex, Clemson University, Clemson, South Carolina 29634-0973, United States

Complete contact information is available at: https://pubs.acs.org/10.1021/acs.analchem.3c04044

Notes

The authors declare no competing financial interest. S.K.W.: Methodology, data curation, visualization, writing — original draft preparation; R.K.M.: conceptualization, supervision, writing — reviewing and editing.

ACKNOWLEDGMENTS

This project was supported in part by National Science Foundation grant CHE-2107882 and the National Institutes of Health grant 1RO1GM141347-01A1.

REFERENCES

- (1) Jayapal, K. P.; Wlaschin, K. F.; Hu, W.; Yap, M. G. Chem. Eng. Prog. 2007, 103 (10), 40.
- (2) De Jesus, M.; Wurm, F. M. Eur. J. Pharm. Biopharm. 2011, 78 (2), 184–188.
- (3) Lai, T.; Yang, Y.; Ng, S. K. Pharmaceuticals (Basel) 2013, 6 (5), 579-603.
- (4) Wurm, F. M. Nat. Biotechnol. 2004, 22 (11), 1393-1398.
- (5) Ha, T. K.; Kim, D.; Kim, C. L.; Grav, L. M.; Lee, G. M. Biotechnol. Adv. 2022, 54, No. 107831.
- (6) Ritacco, F. V.; Wu, Y.; Khetan, A. Biotechnol. Prog. 2018, 34 (6), 1407–1426.
- (7) Shukla, A. A.; Hubbard, B.; Tressel, T.; Guhan, S.; Low, D. J. Chromatogr. B 2007, 848 (1), 28-39.
- (8) Gronemeyer, P.; Ditz, R.; Strube, J. Bioeng. 2014, 1 (4), 188-
- (9) Ladisch, M. R. Bioseparations Engineering: Principles, Practice, and Economics; Wiley-Interscience, 2001.
- (10) Carta, G.; Jungbauer, A. Protein Chromatography: Process Development and Scale-Up; 2nd ed., Wiley-VCH Verlag GmbH, 2020.
- (11) Jendeberg, L.; Nilsson, P.; Larsson, A.; Denker, P.; Uhlén, M.; Nilsson, B.; Nygren, P.-Å. J. Immunol. Methods 1997, 201 (1), 25–34.
- (12) Hober, S.; Nord, K.; Linhult, M. J. Chromatogr. B 2007, 848 (1), 40-47.
- (13) Shi, R. L.; Xiao, G.; Dillon, T. M.; Ricci, M. S.; Bondarenko, P. V. *MAbs* **2020**, *12* (1), 1739825.
- (14) Urmann, M.; Graalfs, H.; Joehnck, M.; Jacob, L. R.; Frech, C. *MAbs* **2010**, 2 (4), 395–404.
- (15) Goyon, A.; Fekete, S.; Beck, A.; Veuthey, J. L.; Guillarme, D. J. Chromatogr. B: Anal. Technol. Biomed. Life Sci. 2018, 1092, 368–378.
- (16) Bulcha, J. T.; Wang, Y.; Ma, H.; Tai, P. W. L.; Gao, G. Signal Transduct. Target. Ther. **2021**, 6 (1), 53.
- (17) Naso, M. F.; Tomkowicz, B.; Perry, W. L., 3rd; Strohl, W. R. *BioDrugs* **2017**, 31 (4), 317–334.
- (18) Milone, M. C.; O'Doherty, U. Leukemia 2018, 32 (7), 1529–1541.
- (19) Tenchov, R.; Bird, R.; Curtze, A. E.; Zhou, Q. ACS Nano 2021, 15 (11), 16982–17015.

- (20) Kourembanas, S. Annu. Rev. Physiol. 2015, 77 (1), 13-27.
- (21) Janouskova, O.; Herma, R.; Semeradtova, A.; Poustka, D.; Liegertova, M.; Malinska, H. A.; Maly, J. Front. Mol. Biosci. 2022, 9, No. 846650, DOI: 10.3389/fmolb.2022.846650.
- (22) Zhang, M.; Hu, S.; Liu, L.; Dang, P.; Liu, Y.; Sun, Z.; Qiao, B.; Wang, C. Signal Transduct. Target. Ther. 2023, 8 (1), 124.
- (23) Li, M.; Li, S.; Du, C.; Zhang, Y.; Li, Y.; Chu, L.; Han, X.; Galons, H.; Zhang, Y.; Sun, H.; et al. Eur. J. Med. Chem. 2020, 207, No. 112784.
- (24) Rezaie, J.; Feghhi, M.; Etemadi, T. Cell Commun. Signal. 2022, 20 (1), 145.
- (25) Shahabipour, F.; Barati, N.; Johnston, T. P.; Derosa, G.; Maffioli, P.; Sahebkar, A. J. Cell. Physiol. 2017, 232 (7), 1660–1668.
- (26) Théry, C.; Amigorena, S.; Raposo, G.; Clayton, A. Curr. Protoc. Cell Biol. 2006, 30, 3 DOI: 10.1002/0471143030.cb0322s30.
- (27) Sancho-Albero, M.; Medel-Martínez, A.; Martín-Duque, P. RSC Adv. 2020, 10 (40), 23975–23987.
- (28) Farzanehpour, M.; Miri, A.; Alvanegh, A. G.; Gouvarchinghaleh, H. E. Biochem. Pharmacol. 2023, 212, No. 115555.
- (29) Kim, S. M.; Yang, Y.; Oh, S. J.; Hong, Y.; Seo, M.; Jang, M. J. Controlled Release 2017, 266, 8–16.
- (30) Gulei, D.; Berindan-Neagoe, I. Mol. Ther. Nucleic Acids 2019, 17, 448-451.
- (31) McAndrews, K. M.; Xiao, F.; Chronopoulos, A.; LeBleu, V. S.; Kugeratski, F. G.; Kalluri, R. Life Sci. Alliance 2021, 4 (9), No. e202000875.
- (32) Xu, Q.; Zhang, Z.; Zhao, L.; Qin, Y.; Cai, H.; Geng, Z.; Zhu, X.; Zhang, W.; Zhang, Y.; Tan, J.; et al. *J. Controlled Release* **2020**, 326, 455–467.
- (33) Usman, W. M.; Pham, T. C.; Kwok, Y. Y.; Vu, L. T.; Ma, V.; Peng, B.; Chan, Y. S.; Wei, L.; Chin, S. M.; Azad, A.; et al. *Nat. Commun.* **2018**, *9* (1), 2359.
- (34) Heath, N.; Grant, L.; De Oliveira, T. M.; Rowlinson, R.; Osteikoetxea, X.; Dekker, N.; Overman, R. Sci. Rep. 2018, 8 (1), 5730.
- (35) Estes, S.; Konstantinov, K.; Young, J. D. Curr. Opin. Biotechnol. **2022**, 77, No. 102776.
- (36) Skrika-Alexopoulos, E.; Mark Smales, C. Biotechnol. Lett. 2023, 45 (4), 425–437.
- (37) Muller, L.; Hong, C. S.; Stolz, D. B.; Watkins, S. C.; Whiteside, T. L. J. Immunol. Methods 2014, 411, 55-65.
- (38) Gupta, S.; Rawat, S.; Arora, V.; Kottarath, S. K.; Dinda, A. K.; Vaishnav, P. K.; Nayak, B.; Mohanty, S. Stem Cell Res. Ther. 2018, 9 (1), 180.
- (39) Gámez-Valero, A.; Monguió-Tortajada, M.; Carreras-Planella, L.; Franquesa, M. l.; Beyer, K.; Borràs, F. E. Sci. Rep. **2016**, 6 (1), 33641.
- (40) Lobb, R.; Möller, A. Methods Mol. Biol. 2017, 1660, 105-110.
- (41) Chen, J.; Xu, Y.; Lu, Y.; Xing, W. Anal. Chem. 2018, 90 (24), 14207–14215.
- (42) Brown, P. N.; Yin, H. Methods Mol. Biol. 2017, 1660, 91-103.
- (43) Rekker, K.; Saare, M.; Roost, A. M.; Kubo, A.-L.; Zarovni, N.; Chiesi, A.; Salumets, A.; Peters, M. Clin. Biochem. **2014**, 47 (1), 135–138
- (44) Yakubovich, E. I.; Polischouk, A. G.; Evtushenko, V. I. *Biochem.* (Mosc.) Suppl. A: Membr. 2022, 16 (2), 115–126.
- (45) Weng, Y.; Sui, Z.; Shan, Y.; Hu, Y.; Chen, Y.; Zhang, L.; Zhang, Y. Analyst 2016, 141 (15), 4640–4646.
- (46) Nelson, D. M.; Marcus, R. K. Anal. Chem. 2006, 78 (24), 8462–8471.
- (47) Wang, L.; Stevens, K. A.; Haupt-Renaud, P.; Marcus, R. K. J. Sep. Sci. 2018, 41 (5), 1063–1073.
- (48) Wang, L.; Marcus, R. K. Biotechnol. Prog. 2018, 34 (5), 1221–1233
- (49) Jiang, L.; Marcus, R. K. Anal. Chim. Acta 2017, 977, 52-64.
- (50) Jiang, L.; Jin, Y.; Marcus, R. K. J. Chromatogr. A 2015, 1410, 200-209.
- (51) Jiang, L.; Marcus, R. K. Anal. Chim. Acta 2017, 954, 129-139.
- (52) Trang, H. K.; Schadock-Hewitt, A. J.; Jiang, L.; Marcus, R. K. J. Chromatog. B: Anal. Technol. Biomed. Life Sci. 2016, 1015, 92–104.

- (53) Trang, H. K.; Marcus, R. K. J. Pharm. Biomed Anal **201**7, 142, 49–58.
- (54) Schadock-Hewitt, A. J.; Marcus, R. K. J. Sep Sci. **2014**, 37 (5), 495–504.
- (55) Jackson, K. K.; Powell, R. R.; Bruce, T. F.; Marcus, R. K. Anal. Bioanal. Chem. **2020**, 412 (19), 4713–4724.
- (56) Huang, S.; Wang, L.; Bruce, T. F.; Marcus, R. K. Biotechnol. Prog. 2020, 36 (5), No. e2998.
- (57) Randunu, K. M.; Dimartino, S.; Marcus, R. K. J. Sep. Sci. 2012, 35 (23), 3270–3280.
- (58) Bruce, T. F.; Slonecki, T. J.; Wang, L.; Huang, S.; Powell, R. R.; Marcus, R. K. Electrophoresis 2019, 40 (4), 571–581.
- (59) Wang, L.; Bruce, T. F.; Huang, S.; Marcus, R. K. Anal. Chim. Acta 2019, 1082, 186-193.
- (60) Huang, S.; Ji, X.; Jackson, K. K.; Bruce, T. F.; Lubman, D. M.; Marcus, R. K. Anal. Chim. Acta 2021, 1167, No. 338578.
- (61) Billotto, L. S.; Jackson, K. K.; Marcus, R. K. Sep. 2022, 9 (9), 251-264.
- (62) Jackson, K. K.; Powell, R. R.; Bruce, T. F.; Marcus, R. K. Analyst **2021**, 146 (13), 4314–4325.
- (63) Jackson, K. K.; Mata, C.; Marcus, R. K. Talanta 2023, 252, No. 123779.
- (64) Jackson, K. K.; Marcus, R. K. Electrophoresis **2023**, 44, 190–202, DOI: 10.1002/elps.202200149.
- (65) Bruce, T. F.; Slonecki, T. J.; Wang, L.; Huang, S.; Powell, R. R.; Marcus, R. K. *Electrophor.* **2019**, *40* (4), 571–581.
- (66) King, H. W.; Michael, M. Z.; Gleadle, J. M. BMC Cancer 2012, 12 (1), 421.
- (67) Beninson, L. A.; Fleshner, M. Semin. Immunol. 2014, 26 (5), 394-401.
- (68) Minh, A. D.; Kamen, A. A. Vaccines 2021, 9 (8), 823.
- (69) Randunu, K. M.; Marcus, R. K. Anal. Bioanal. Chem. 2012, 404 (3), 721-729.
- (70) Wang, L.; Trang, H. K.; Desai, J.; Dunn, Z. D.; Richardson, D. D.; Marcus, R. K. *Anal. Chim. Acta* **2020**, *1098*, 190–200.
- (71) Fausnaugh, J. L.; Pfannkoch, E.; Gupta, S.; Regnier, F. E. Anal. Biochem. 1984, 137, 464–472.
- (72) McCue, J. T. Meth. Enzymol. 2009, 463, 405-414.
- (73) Mazzer, A. R.; Perraud, X.; Halley, J.; O'Hara, J.; Bracewell, D. G. J. Chromatogr. A **2015**, 1415, 83–90.
- (74) DeLano, W. L.; Ultsch, M. H.; de, A. M.; Vos; Wells, J. A. Science 2000, 287 (5456), 1279-1283.
- (75) Deisenhofer, J. Biochem. 1981, 20 (9), 2361-2370.
- (76) Pirok, B. W. J.; Stoll, D. R.; Schoenmakers, P. J. Anal. Chem. **2019**, 91 (1), 240–263.
- (77) Stoll, D. R.; Carr, P. W. Anal. Chem. 2017, 89 (1), 519-531.
- (78) Pepaj, M.; Wilson, S. R.; Novotna, K.; Lundanes, E.; Greibrokk, T. J. Chromatogr. A **2006**, 1120 (1-2), 132-141.
- (79) Vanhoenacker, G.; Vandenheede, I.; David, F.; Sandra, P.; Sandra, K. Anal. Bioanal. Chem. 2015, 407 (1), 355–366.
- (80) Huang, S.; Wang, L.; Bruce, T. F.; Marcus, R. K. Anal. Bioanal. Chem. 2019, 411, 6591–6601.
- (81) Keysberg, C.; Hertel, O.; Schelletter, L.; Busche, T.; Sochart, C.; Kalinowski, J.; Hoffrogge, R.; Otte, K.; Noll, T. *Appl. Microbiol. Biotechnol.* **2021**, *105* (9), 3673–3689.
- (82) Belliveau, J.; Papoutsakis, E. T. Biotechnol. Bioeng. 2022, 119 (5), 1222-1238.
- (83) Meyer, H.-P.; Minas, W.; Schmidhalter, D. Industrial Scale Fermentation. In *Industrial Biotechnology: Products and Processes*, Wittmann, C.; Liao, J. C., Eds.; Wiley-VCHVerlag KGaA, 2017.
- (84) Billotto, L. S.; Jackson, K. K.; Marcus, R. K. Separations 2022, 9 (9), 251–264.